Department of Precision and Microsystems Engineering

TITLE: An improved chip design for Nanomotion Detection

NAME: Shunyu Yao

Report no : 2023.009
Coach : ir.Irek Roslon, dr.ir.Aleksandre Japaridze
Professor : prof.dr.Farbod Alijani
Specialisation : Dynamics of Micro and Nanosystems
Type of report : Master Thesis
Date : 10 February 2023

Delft University of Technology

Department of high tech engineering

An improved chip design for Nanomotion Detection

Master Thesis

Author:
Shunyu Yao 5249090

Professor:
prof.dr.Farbod Alijani
Supervisors:
ir.Irek Roslon
dr.ir.Aleksandre Japaridze

Contents

List of Figures

List of Tables

Abstract

Antibiotic susceptibility test (AST) shows the efficacy of antibiotics against different strains and is frequently applied in finding new antibiotics, bacteria identification, and clinical analysis. The tests provide scientific evidence for finding pathogens and avoiding the misuse of antibiotics.

The first AST was invented by Alexander Fleming in the 1920s, right after the invention of antibiotics. Since then, methods of antibiotic testing have developed and improved. The nanomotion method is one of the auspicious methods in antibiotic susceptibility tests (AST). It features detecting the vibration of single living bacteria on the graphene drum before and after being treated with antibiotics. However, such a method is restricted in laboratory conditions currently. The aim of this thesis is to make the nanomotion method compatible with clinical requirements. As a result, a new set of designs including chips and their cartridge is fabricated and validated in this thesis.

In this research, a review including the traditional and up-to-date AST methods shows that in the nanomotion method, only one measurement is carried out simultaneously. As the research question, this novel design is supposed to carry out a few measurements with different parameters including concentration and antibiotic category.
To realize this purpose, concept designs analyzing the requirements are carried out on three components, fluid system, ventilation and sealing. More parameters regarding the material and fabrication are discussed in order to ensure its requirements including durability, printing quality and more.
In the end, the design is validated and tested in the setup. The result is compared to the original nanomotion method and the traditional AST method. We hope the thesis provides the possible direction of improvements for the nanomotion method.

Chapter 1

Introduction to Antibiotic susceptibility test

As the first chapter of the thesis, the introduction will enumerate a few AST methods from the traditional disc diffusion method to the up-to-date ones. Among the novel method, the nanomotion one is regarded as the focus of the thesis and a research question is raised to improve the method in compatibility and automation.

1.1 Antibiotic Susceptibility Test

Antibiotics were believed to be the most effective substance against bacteria, saving millions of lives from inflammation and infection. However, the misuse of antibiotics contributes greatly to the creation of bacteria with antibiotic resistance[9]. The variation of the bacteria in antibiotic resistance calls for research in two different directions. Antimicrobial resistance(AMR) concentrates on the mechanism of the resistance and previewing for new antibiotics. The antibiotic susceptibility test (AST), which is the main focus of the thesis, aims at finding novel methods with affordable and rapid features.

1.1.1 Traditional AST methods

Disc diffusion method At present, the disc diffusion method is most commonly adopted in antibiotic susceptibility tests [1]. The bacteria are swabbed on the agar and the antibiotic discs are placed on top. The antibiotic diffuses from the disc into the agar in decreasing amounts the further it is away from the disc. If the pathogen is killed or inhibited by the concentration of the antibiotic, there will be no growth in the immediate area around the disc. A picture of the disc diffusion method is shown in figure 1.1.

The bacteria sample must grow for 16-24h before forming a recognizable colony according to the standard [10]. When it comes to clinical analysis, the test should be as fast as possible. Considering the common procedure of outpatient, it is expected to receive a result within a workday, preferably less than 6 hours. According to the previous discussion, the disc diffusion method requires 16-24h time to incubate and receive an observable result. To make matters worse, it takes manpower to examine the colony on the disc which is rather laborious. The

disadvantage of the traditional method calls for novel methods to finish the measurement in 8-hour work shift.

It should be noticed that the method could only analyze if the pathogen is susceptible to the antibiotic qualitatively. The suitable antibiotic concentration which could kill the bacteria efficiently while avoiding the misuse of antibiotics is still unknown to us all. To analyze the suitable concentration of antibiotics, the broth dilution method will play an important role.

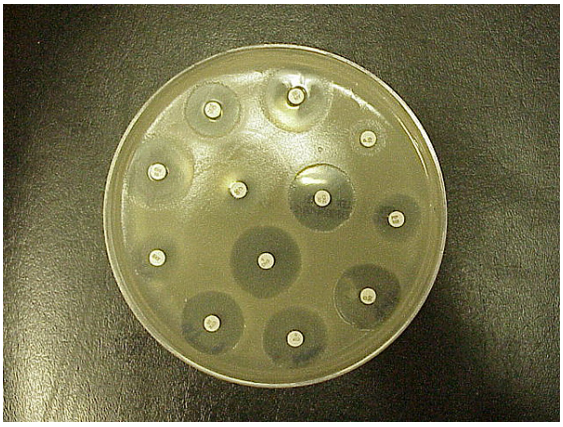

Figure 1.1: Petri dish of 88mm in diameter containing discs of antibiotics on an agar plate of bacteria. Circular zones of poor bacterial growth surround some discs, indicating susceptibility to the antibiotic. [1]

Broth dilution method The broth dilution method is another common method adopted in clinical diagnosis. It is used to determine the minimum inhibitory concentration (MIC) of antibiotics. The antibiotic is diluted in sterile broth to a series of different concentrations. Then the dilution is mixed with broth inoculated with a known number of bacteria. The lowest concentration without visible growth of bacteria is regarded as MIC. The concentration result corresponds with the interior side of the boundary between the bacteria colony and the inhibited area which in figure 1.1. By comparing the MIC of different samples against different antibiotics, the efficacy of antibiotics and the susceptibility of bacteria is identified.

The suggested dilution range of different antibiotics is given by the clinical standard. Traditionally, the antibiotic is diluted according to the rule of doubling dilution. For example, if the suggested dilution range is $0.25 - 128mg/L$. The groups of concentration should be 128, 64, 32, 16, 8, 4, 2, 1, 0.5, 0.25 and 0 mg/L.[1]

1.1.2 Automated method

As we have mentioned in previous paragraphs, neither of the traditional method mentioned above features automatic traits. Technicians have to finish the preparation, inoculation, and measurement by themselves. The workload increases as the number of samples increases. As a result, the testing process is tiring and error-prone. Hence, novel commercial methods are introduced in this paragraph with automation adaptation.

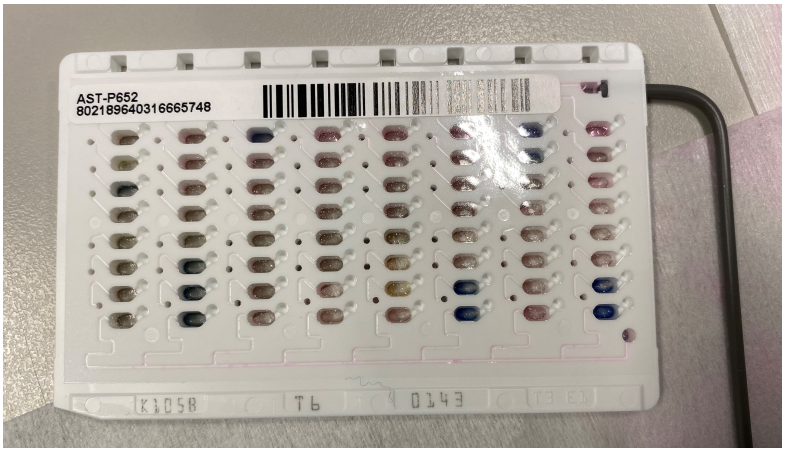

Figure 1.2: A picture of a Vitek card. The array of cavities containing various antibiotics and indicators is connected by a complex microfluid system. The channels are dyed pink by the author for better contrast. Grey tube functions as the inlet. The cavities with various indicators feature different colors.

Vitek cards As is shown in figure 1.2, the Vitek card is produced by bioMerieux for clinical diagnosis. The main structure of this card is made of plastic where arrays of oval cavities and microfluid channels are carved on both sides. To seal the cavities and channels, transparent plastic membranes cover the surface of the card. A grey inlet connects to the microfluid channel. The working procedure is simple: submerge the grey inlet into the bacteria suspension, and place the card in high air pressure, the liquid will enter the cavities by capillary and pressure difference.

After adding the suspension of bacteria, the freeze-dried antibiotics which were stored inside the cavities when fabricated are dissolved. The growth of bacteria results in the variation of turbidity[11]. By measuring the turbidity using a photometer, the susceptibility is determined.

Phoenix Card Apart from Vitek, BD company has its susceptibility test panel called Phoenix card. Figure 1.3 shows the structure of the Phoenix card with 3 layers. The bottom layer features wells of 2 mm in diameter in which crystallized indicators and antibiotics are placed during fabrication. Two sets of serpentine microfluid channels, one for identification and one for AST, and a reservoir with a sponge compose the middle layer in black. The top layer is welded with the bottom layer in order to seal the panel.

When testing, around 8 ml suspension of bacteria is poured from the two round inlets on the upper part. The liquid flows through the zig-zag channel and fulfills the wells while the excess liquid is absorbed by the white sponge in the reservoir. After adding liquid, the inlet is clogged and the panel is placed upright. Then the bacteria are incubated and the wells are examined for turbidity and colorimetric change in a specific instrument from the same company. By observing bacteria growth, it requires around 16 hours to receive a trustworthy result [11].

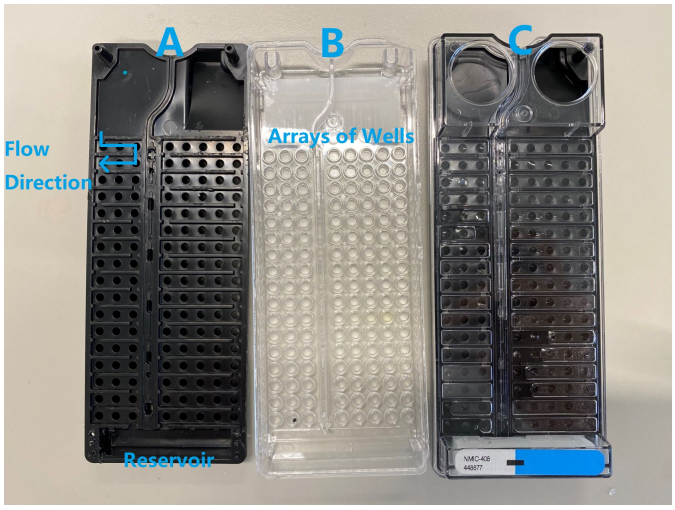

Figure 1.3: A picture of an opened and an intact BD panel. A: The middle layer, directions of fluid flow are marked by arrows; B: the bottom layer with arrays of wells; C: an intact panel.

1.1.3 Cantilever method

Although commercial techniques enable automatic AST, it still requires bacteria growth before adding the sample to the setup to distinguish the efficacy of antibiotics. Hence, a novel method called the cantilever method requiring fewer bacteria is illustrated here.

In 2013, Longo et al[2] found out that living organisms attached to a cantilever could induce nanoscale oscillations. The setup of the experiment is simple. The bacteria sample is attached to the tip of an AFM cantilever. The tip is inserted into an analysis chamber filled with growth medium. The movement of the bacteria results in the oscillation of the cantilever. The magnitude of the oscillation is measured by a reflected laser beam focused on the tip of the cantilever. These effects vary as the medium solution changes in the chamber. A schematic representation of the set-up is shown in figure 1.4

Afterward, more research [12] [13] [14] [15] [16] [17] reveals that the cantilever method is feasible with most kinds of bacteria and related antibiotics. The experiments include fast and slow-growing bacteria, motile and non-motile strains, and Eukaryotatic cells.

Compared to the traditional method, the cantilever method does not have to incubate the sample for a long period to wait for the bacteria to form a colony. It only needs a small aliquot of 10^5 bacteria to have a measurable signal[2] compared to 150 million cells per mL in the disc diffusion method. In conclusion, the cantilever method proves to be successful in detecting oscillation signals of slow-growing bacteria and identifying the MIC and MBC of certain antibiotics.

1.1.4 Nanomotion method for single bacteria

The cantilever method still has its drawback. Although the setup requires 10^5 bacteria cells compared to around 150 million cells per microliter in disc diffusion method, only hundreds of bacteria manage to fix themselves on the tip and contribute to the oscillation of the cantilever.

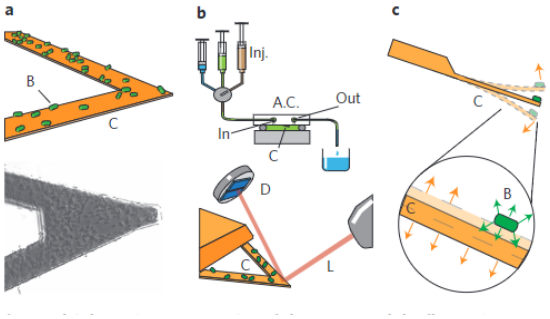

Figure 1.4: Schematic representation of the set-up and the fluctuating cantilever. A) Top: Illustration of the cantilever (C) with living bacteria (B). Bottom: cantilever under optic microscope. B) Top: Cantilever in the acquisition chamber (A.C.), which is flushed by different liquids through the injection system (Inj.).The chamber is equipped with input (In) and output (Out) tubes for changing the media. Bottom: A laser beam (L) is focused on C. Its reflection is collected by a detector (D). The oscillation of cantilever will result in reflect beam path changes. C) Sketch of the fluctuations of C produced by B on the surface.[2]

Incubation is still necessary for the replication of samples to receive strong enough signals and for the binding progress to the cantilever tip. To overcome such a problem, fewer bacteria should be attached to the sensor and the sensitivity should be improved. To enhance the sensitivity of the sensor, Irek et al [3] present a novel single-cell technique based on a suspended graphene membrane.

The substrate is designed to be a 5*5 mm^2 silicon chip with a 285 nm layer of silicon oxide with round hole patterns on it. The diameter of the holes ranges from 4 to 8 μm, longer than the average length of the experimental *E.coli* strain. A layer of graphene was transferred to the surface of the chip by a copper sheet. Then the chip is sealed in a cuvette for inspection and experiment later.

The bacteria *E.coli* is cultivated in LB media and treated with APTES to bind the bacteria to the suspended graphene layer. Then the suspension is filled into the cuvette with the chip. The chamber is left for 15 minutes in a horizontal position to deposit the bacteria on the surface. Some of the bacteria will bind to the chip and the others will fall to the bottom of the cuvette. The bacteria which are fixed in the middle of the cavity will generate graphene oscillation when they move their flagella and carry out other metabolism activities like material transport through the cell membrane. Because of the suitable diameter of the cavity, one bacterium lies in one cavity in most cases. A few cavities are found empty but none are filled with multiple bacteria. Afterward, the sample is examined under Keyence optical microscope and then the optical nanomotion setup as shown in figure 1.5 Oscillation of each drum is recorded for thirty seconds. After that, antibiotics are added and the sample is measured for a new round.

Providing insight into the nanomotion of single bacteria, this novel method features a shorter analysis time. The main factors that influence the analysis time include the required time antibiotic takes effect and the number of cavities[3]. Generally, 4-6 hours are sufficient to finish the analysis and for some instant-effect antibiotics, 1 hour would be enough. Compared to the cantilever method, the nanomotion method requires fewer bacteria and saves time from

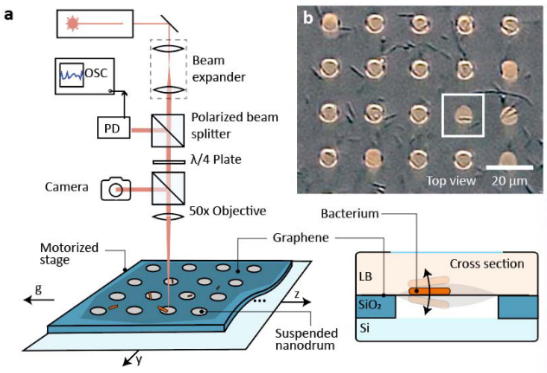

Figure 1.5: Detection of nanomotion of single bacteria by graphene drums. a) Illustration of the optic measurement setup used to detect the nanomotion. The laser beam is reflected from the graphene drum and the oscillation of the laser beam represents the movement of the bacteria on the drum. b) Optical microscope image of an array of suspended drums with adhered E. coli.[3]

incubating samples. Also, the single bacteria measurement is repeated in different cavities on the same chip, which greatly increases the reliability of the result. In addition, the testing material changes from expensive cantilever tips to silicon chips, making standardization and clinical application possible.

1.2 Summary and Problem Definition

The nanomotion method features fewer bacteria and little incubation time according to the previous introduction of the AST methods. However, when compared to the up-to-date commercial product, it is less automated and requires more in-hand time for technicians. To make matters worse, when the bacteria strain requires AST against different antibiotics of different concentrations, which is often the clinical case facing an unknown pathogen, the technician has to replace the chip with a new one and refill the environment with the specified antibiotic a few times, making the measurement extremely long.

Based on the comparison and analysis above, the research question driving this project is defined as how to carry out the parallel nanomotion AST with different antibiotics and concentrations at one measurement.

To realize this purpose, the following chapters of the thesis will be carried out in the following way. Firstly, the design will be divided into several parts based on the main functions. Solutions based on literature reviews and competitors are listed and compared. . After determining the concept of different parts, prototypes are fabricated, overcoming obstacles in material, the bonding method, and critical parameters. The validation and the performance of the model will be found in chapter 3. Chapter 4 concludes and analyzes the result and looks forward to possible improvements in the future.

Chapter 2

Cartridge design for parallelizing nanomotion detection

To answer the research question, the first part will analyze the requirements and carry out the concept design in the sequence of different components. The schematic of the design is concluded in the second part. After the concept design, the last part will focus on the challenges and requirements during the fabrication. The prototype will be fabricated with adjustments in view of practical obstacles of material, bonding, and parameters.

2.1 Component analysis and Concept design

This design is supposed to fulfill several functions. The fluid system is supposed to create environments with different concentrations and distribute the suspension of bacteria to the environments. Apart from the fluid system, the design has to deal with the air bubbles inside the cartridge with an air channel. Besides, the cartridge should be sealed properly for storage and optical measurement. The design should function properly with all these requirements. The following paragraph will analyze the requirements from the 3 aspects mentioned above and compare the possible solutions to the challenges.

2.1.1 Fluid system

The fluid system consists of two main functions: antibiotic environment creation and liquid distribution. The first function, environment creation, stands for how the chip will be saturated in the antibiotics and the second function, liquid distribution, will discuss how to provide the necessary liquid to the chips. There are several candidate solutions for the two functions as figure 2.1 illustrates and either combination of the two functions composes of a solution to the total fluid system.

The creation and separation of antibiotic environment In the first part of this section, we are going to discuss how to create antibiotic environments of certain concentrations for measurement. For example, if a sample needs to be tested against 3 antibiotics and a range of concentrations in one cartridge design, what will the design be like? Should we apply structures on the chip with graphene or build a chamber around it? In general, to saturate the chips in

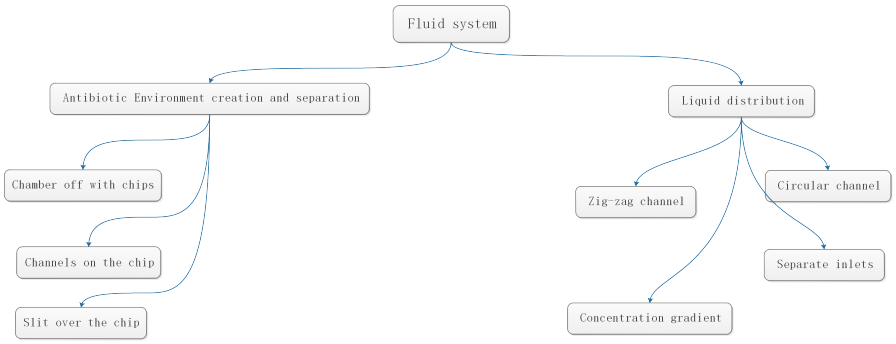

Figure 2.1: The possible concept design of the two functions in fluid system. The fluid system is supposed to complete two important tasks, one is liquid distribution, another is antibiotic environment creation. The possible concept designs are listed in the figure. Either combination of the two sub-function will be a full design of the fluid system part.

different antibiotic solutions without cross-contamination, there are 3 ideas. The first idea is to build a chamber for each environment. The chips are glued at the bottom of the chamber. Before measuring, suspension of bacteria and antibiotics are injected into the chambers, creating the necessary measurement environment. An illustration of such a design is shown in figure 2.2.

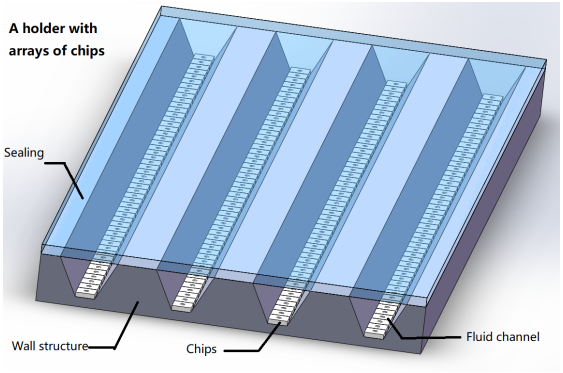

Figure 2.2: The holder is divided into several columns and different concentrations of antibiotic flow through each column. In each column, a few chips with cavities are glued inside the chamber. The chip is represented by a single round cavity and a square outline.

Different from the previous one, not only can we separate chips with different chambers, but it is also feasible to divide the cavities on one chip into several sections as well. As figure 2.3 shows, wall structures are designed on the chip to separate the cavities in several columns, providing isolation of different concentration environments.

According to Japaridze's research in 2017, a transparent cover with slits made from PDMS is designed for confining circular DNAs in channels of different widths [18]. Similarly, in figure 2.4, we can adopt this transparent cover over the chip to divide the cavities into several columns.

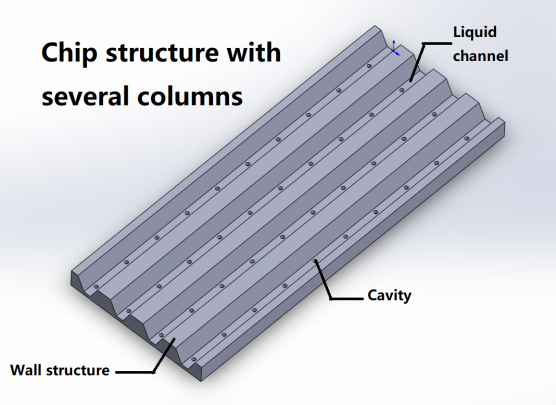

Figure 2.3: The chip is divided into several columns by wall structures and different concentrations of antibiotic flow through each column, creating different environments for bacteria. In each column there are cavities with graphene for measuring

The three novel ideas, the chip chamber, the chip with walls, and the cover with slits have their unique limits and advantages. The two on-chip designs feature a tiny scale and require less liquid while the off-chip design has a regular size which is handier for clinical diagnosis. From the point of fabrication, the chip with wall design has the greatest difficulty in applying graphene membrane. Usually, the graphene is transferred to the chip by chemical vapor deposition (CVD) or mechanical stamping. Both of the techniques require a flat surface without protruding structures. In addition, the graphene membrane is fragile and the cover design with slits may destroy the graphene while connecting with the substrate chip.

The workload for the 3 designs is similar, all 3 designs have two parts sealed together. The only difference is that the two designs that work on the chip feature a small scale of micrometers. The two parts should be carefully aligned in case of leakage and the sealing process requires more attention from technicians compared to the regular-size design with chambers containing chips.

Leakage is another problem taken into consideration. The idea of slits covering the chip has the worst performance in leakage because it is difficult to secure a reliable bonding over a layer of graphene drum without damaging it. The two other methods feature similar performance on leakage if bonded properly.

The morphological table of the three ideas is shown in table 2.1. Four criteria from the requirements of the design are adopted to evaluate the performance of the solutions from 1 (bad) to 5 (good). The criteria include the difficulty in fabrication, the workload for technicians, performance in leak-tight, and the amount of liquid used. All the reasons of marks have been explained in the previous paragraphs.

Liquid distribution Another function of the fluid system of the design is to distribute the desired amount of liquid including antibiotic and bacteria samples to the environment around the chip. For this function, 4 solutions are explained and discussed in this section, zig-zag channel, circular channel, separate channel, and concentration gradient channel.

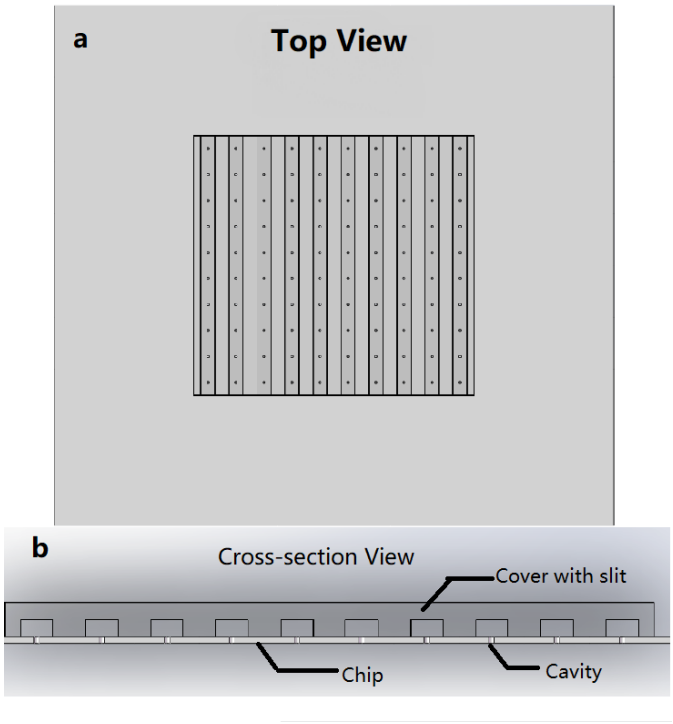

Figure 2.4: An illustration of chip design with PDMS slit. A) An overview of the chip model with a transparent slit. B) A cross-section view of the chip's center area. The slit separates the arrays of cavities in parallel.

The first idea is to place the freeze-dried antibiotic first inside the chambers and a zig-zag channel connecting all the environments will guide the suspension of bacteria flushing into the environment later. By calculating the amount of antibiotic and the volume of the chambers, the desired concentrations are established in the cartridge.

A more complex design of circular distribution was given by Yang et al [4] in 2011. As shown in figure 2.5, the radial channel network is composed of multi-circle channels and parallel branch channels. The two inlets are in the center of the system. With this amazing design, each branch channel from the outer circle provides combinations of different concentrations of the two added liquids. Based on this geometric and fluidic distribution system, we could create different environments in a circular arrangement in our design. Another simple design is adopted by many microfluidic experiments. As figure 2.7 shows, dedicated inlets and outlets are connected to each measurement environment. Different from the previous method which contains freeze-dried antibiotics, this design prefers to prepare the required broth of different concentrations separately beforehand.

The last idea is to create a concentration gradient by the diffusion of solute. It features two sources with two different liquids connected by a narrow channel. With the slow diffusion of the solute, the concentration of certain particle decrease along the direction of the channel. In our case, the device could easily create a concentration gradient of a certain antibiotic for the coming

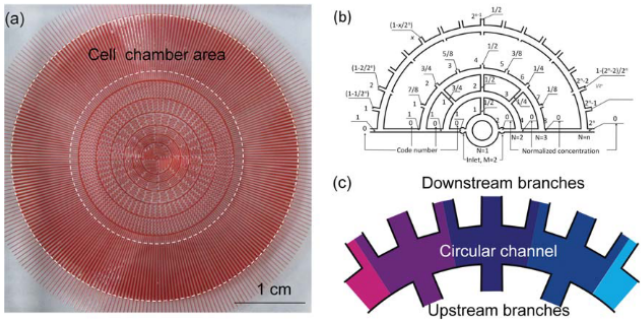

Figure 2.5: (a) Positive master of the 2-inlet chip made of an AZ P4620 photoresist patterned on a glass substrate. (b) Schematic of the 2-inlet gradient generator with one set of gradients (the other part omitted is symmetric with the schematic diagram). (c) Schematic of fluid distribution at the junctions of the branch channels and the circular channel[4]

measurements. The four solutions are compared in table 2.1 against the same requirements. As mentioned before, circular distribution design features several layers of circular channels with many fine inlets between layers. Fabricating such cartridges requires high-resolution lithography machines. When carrying out clinical analysis, two or more source solutions of antibiotic and bacteria suspension with stable flow are necessary to realize the function of creating different antibiotic concentrations, which requires demanding auxiliary equipment in providing source liquid and a mild workload of preparation for technicians. The circular distribution design is highly integrated so little liquid is required to carry out the analysis. Leakage could not happen because of the same reason, integrated design.

As for the design with dedicated inlets and outlets. The fabrication process is no longer an obstacle because the design is simply the multiplication of a simple structure. However, when applying it for clinical use, technicians have to connect the design with a couple of pipelines containing solutions of different antibiotic concentrations without mistakes. The workload of such a task is heavier than the traditional disc diffusion method. With the increase of inlets and outlets, the design requires the most liquid of the 4 candidate methods because of the liquid consumption during flushing. As a design with good compatibility with standard microfluid equipment, the dedicated inlets and outlets seldom leak if treated properly with the suitable connection of mature techniques.

Unlike the previous two designs, the concentration gradient method seems to achieve the balance between fabrication difficulty and workload with an acceptable amount of required liquid. The leakage is the key problem of the design because in some cases, filter membranes are adopted in order to slow down the diffusion process and stabilize the concentration gradient. Heavy leakage of cross-contamination is detected when the membranes expire during the measurement[19]. To make matters worse, like disc diffusion method, the exact MIC of the antibiotic against the specimen is unknown. Only an estimated value can be obtained by calculation based on diffusion speed and the division boundary of bacteria activity.

In the end, the zig-zag channel idea wins out because of its performance. The design is easy to fabricate with a 3D printer and all the technician needs to do is pour in a certain amount of bacteria suspension. If sealed properly, there is no leakage or cross-contamination between

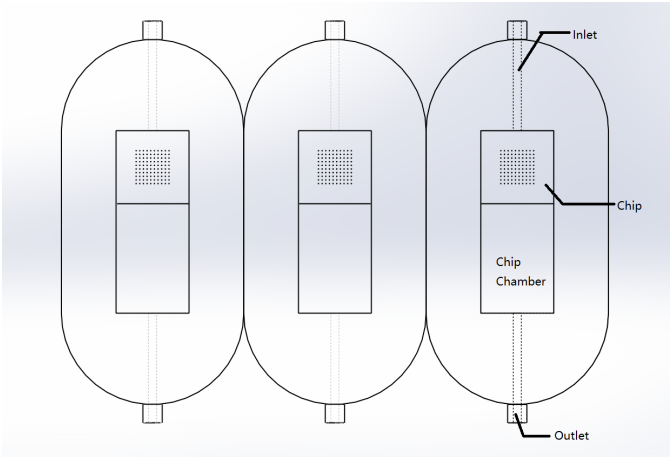

Figure 2.6: Schematic illustrations of a dedicated fluid system for each measurement environment. Three chips were contained in three chambers with dedicated inlets and outlets. For different inlets different concentrations of antibiotics are provided.

different environments. The only disadvantage could be the liquid amount required for the test. With a long zig-zag channel design, it will certainly leave a certain amount of liquid inside the channel and the reservoir which means the design could consume more bacteria suspension than the circular one.

	Solution	Fabrication	Workload	Liquid amount	Leakage	Avg
Environment	Chamber off the chip	5	4	1	4	3.5
	Channels on the chip	1	3	5	4	3.25
	Slit over the chip	2	3	5	1	2.75
Distribution	Zig-zag single channel	5	5	3	5	4.5
	Circular channel	1	3	5	5	3.5
	Separate channel	5	1	2	5	3.25
	Concentration gradient	3	3	3	2	2.75

Table 2.1: The morphology table of fluid system

2.1.2 Bubble formation countering

After fabrication and before adding liquid, the cartridge is empty of liquid but full of air. When adding liquid, the bubbles will try to escape from the design thus blocking the distribution channel or staying inside the cartridge. The serious challenges include blockage of the liquid distribution system and imprecise concentrations.

To deal with the formation of bubbles, a few solutions are introduced in this paragraph. Among them are chimney design, ventilation channel, gaps for air, air chamber and positive pressure.

In chapter 1.2, two commercial AST cards are introduced and they have their specific solution to bubble formation and prevent blockage. The Vitek card, features ancillary equipment to generate positive air pressure outside the cartridge to force the liquid flowing into the cartridge. In addition, the Vitek card has designed an air chamber for each main chamber. In the air chamber stores the compressed air.

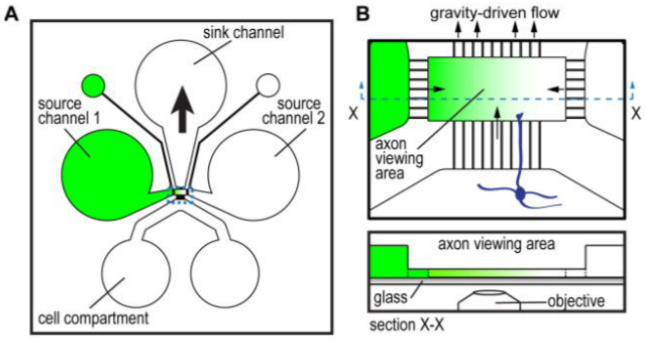

Figure 2.7: (A) Illustration of creating concentration gradient along the channel. Source channels connect to a smaller outlet port to facilitate channel filling. Gradients are established by removing liquid from the sink well. (B) Illustration of the enlarged measurement area and a profile view (bottom).[5]

Apart from the solutions Vitek adopts, BD cards have their specially designed structures to tackle the bubbles. At the top of the cartridge, two chimneys shown in figure 2.18 connect the bottom layer and the inlet reservoir as the ventilation channels. The ventilation channel leads the interior circulation of air and liquid without leakage to the exterior environment. Between the zig-zag channel in the middle layer and the wells in the bottom layer, there is a small gap allowing air to escape outside the wells. Because of bad hydrophilicity of the material, the liquid is prevented from escaping the wells.

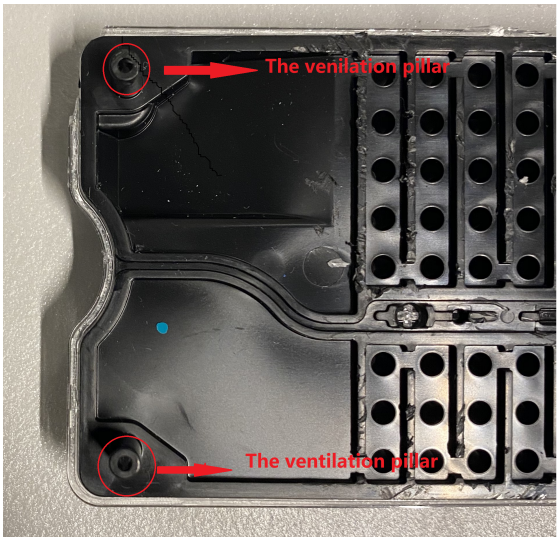

Figure 2.8: The two hollow pillars designed in the middle layer of BD panel. The pillars at the top of the panel are pointed out with red circles. The black pillar is designed in the middle layer connecting the space between the bottom layer and the top layer.

As the last possible method, a specially designed ventilation channel for the design may expel the bubbles and reduce the chance of blockage. The ventilation channel system is designed as shown in the line sketch figure 2.9. Two side channels connect the top and bottom reservoirs. Above each line of chambers, there is a branch channel connecting all the chambers with a small breach. The cross-section area of the breaches is 1*1mm. It is small enough to prevent liquid flow by capillary while allowing the air bubbles to escape.

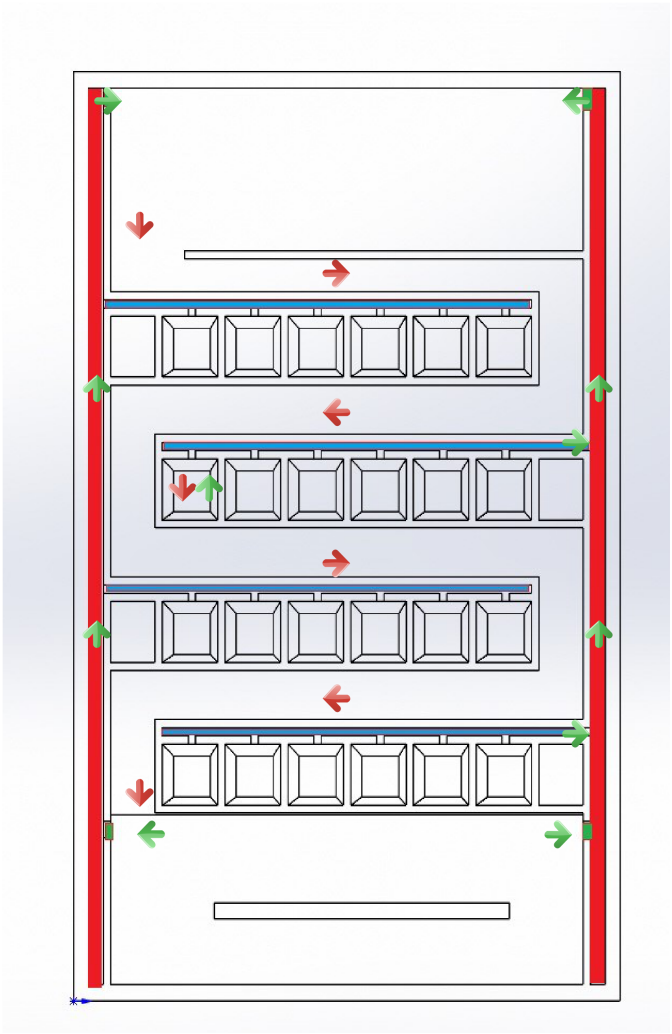

Figure 2.9: The line sketch of the model. The ventilation designs are marked with colors. Red represents the main ventilation channel, blue marks the branch channel and green stands for the connection. The airflow is marked in green arrows and the liquid is marked in red arrows.

The positive pressure and flexible volume method are first ruled out because ancillary equipment and more required material are introduced to the design. The chimney and narrow gap ideas seem feasible but they are designed for a 3-layer device like BD panel. They do not fit the two-layer design in this thesis. In the end, the specially designed ventilation system with two

side channels is determined to be the best option.

2.1.3 Sealing and packaging

The last component of the design is sealing and packaging. This part is a transparent layer bonded over the cartridge to seal the cartridge and allow laser beam shooting to the chips. This component is supposed to firmly seal the design from any leakage and provide compatibility for optical measurement. The challenges require the sealing to be flat and transparent, durable, and no glare.

The first requirement for the sealing is flatness and transparency. It is obvious that only transparent sealing can allow illuminating light and lase for measurement to pass. The sealing of the cartridge features a relatively small contact area and large cavities. The insufficient stiffness of the cartridge and the cover will leads to a cover in bad shape.

If the stiffness of the cover is not enough, sunken areas may be detected on the surface of the cover, resulting in unexpected consequences like errors in the volume of the chamber, and poor signal because of the deflected laser beam. In view of this, cylinders are designed in the top and bottom reservoirs, providing extra support to the cover.

Apart from supporting structures, if the stiffness of the cartridge is not enough, distortion will happen around the contact area of the two components. To solve this problem, thin wall structures are enhanced in thickness to reduce distortion.

The second problem is the durability of bonding. It is a complex problem including material, bonding strategy, and contact area. The combinations will be discussed based on the fabrication of the prototypes and experiments on them in the next part of the thesis.

Besides, glare is another problem needed to solve during the design. It means that the light is reflected between the transparent solid medium and the target, which means the target planar is illuminated by both reflected light and direct light. The glare problem happens frequently with light path penetrating multiphase of reflective material. In our case, the light from the light source has to go through the air, the cover, and liquid to reach the chip, resulting in reflections several times and visions of poor contrast. Without a clear view of the cavities on the chip, there is no chance to calibrate the laser to the cavities and continue the research.

There are several ways to reduce the influence of glare: reducing the liquid layer, less reflective sealing material, and other optical methods like applying polarizers and improved illumination. In this thesis, we will focus on the solutions from the aspects of cartridge design rather than the optics improvement of the setup.

In this section, solutions to sealing and packaging are mentioned while no concept designs have been determined. This is because the solutions to this design are closely related to detailed parameters and material selection. After summarizing the general schematic of the design in the following section 2.2, the material selection and other matters concerning fabrication will be fully discussed with proof of experiments in the following section 2.3 about fabrication.

2.2 Schematic of the cartridge and its main components

To summarize the concept design, the full design of two parts, the cartridge, and the cover is illustrated here. The concept model of the cartridge is shown in figure 2.10. Arrays of chambers are arranged in the middle of the cartridge. A serpentine liquid fluid channel flows around the chambers, connecting each chamber with an arch-shaped entrance. The cartridge has two reservoirs placed at the top and bottom. The top one functions as the inlet and the bottom one stores the excess liquid.

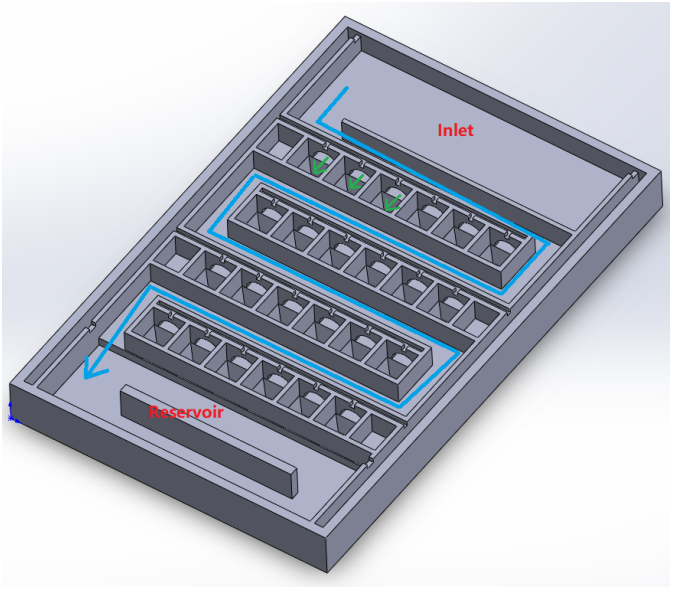

Figure 2.10: The model of the cartridge. The liquid flow is illustrated with blue and green arrows.

The chamber is designed in the shape of an inverted frustum of which the bottom section size is the same as the chip size, making placing and positioning the chip more precise and convenient.

The cover is a transparent sheet material that seals the cartridge while allowing optical measurement. It is supposed to have the same width and length as the cartridge with a liquid inlet. It is a very flexible part because the only function of this transparent cover is to seal the cartridge. Because of this, the width and length of the cover will be the same as the cartridge's size. The width and length of the cover are increased by 1mm Considering the error in installation and assembly.

The ventilation channels are the shallow channels fabricated around the chambers and cartridges. They will be analyzed thoroughly in the following paragraphs.

While using the cartridge, freeze-dried antibiotics should be placed in each chamber with the required amount before sealing the cartridge with the cover. Before measuring, a certain amount of bacteria suspension is poured in from the inlet and the antibiotics in the chambers are diluted

to specific concentrations. The bacteria will bind to the graphene membrane and oscillation can be detected about one hour after pouring.

2.3 Set-up design and fabrication

According to the previous discussion, the components of the design are analyzed and the challenges of what the fluid system will be like and how to avoid the formation of bubbles are explained and solved. In this part of the chapter, prototypes are fabricated and some challenges during the fabrication, including material selection, bonding strategy, and critical dimensional parameters will be taken into consideration in this section.

2.3.1 Material selection for cartridge

As a prototype of the design, the cartridge is planned to be 3D-printed. Candidate material includes PLA, resin and PETG.

Polylactic acid (PLA) material is a very commonly used material in 3D printing. In our lab, it is printed from a Prusa slicer MK3 3D-printing machine with a resolution of 0.1-0.2mm and a 25×21×21 cm building volume. Polyethylene terephthalate glycol (PETG) is another optional material for the Prusa slicer. It is half-transparent material with a higher stiffness when compared to PLA.

Unlike the previous two materials, the resin (HTM-120) is printed by stereolithography 3d printer from Envisiontec. The printer has a higher resolution with a smaller volume of 45 x 28 x 100 mm.

2.3.2 Material selection for cover

There are many choices in finding a transparent sheet material for the cover. Polydimethylsiloxane (PDMS) is commonly used in microfluid design because its perfect biology compatibility and formability. It can be designed into any shape with a mold and curing process.

Poly(methyl methacrylate) (PMMA) is another transparent optional material for fabricating the cover. The sheet material of PMMA can be easily processed into any 2D design by laser cutting.

The last candidate is glass. It is hard but brittle with little bonding methods.

2.3.3 Bonding strategy

The bonding is supposed to combine the cartridge and the cover together and the bonding strategy varies when the material of the two parts changes. A few feasible methods of the materials mentioned in the previous two chapters are mentioned here.

The most simple and versatile method should be thermal bonding. On heating to the melting point, the cartridge and the cover will melt. If compressed, the crosslink between the two materials will generate a firm bonding. The restriction of this method is that only materials with similar melting points can be bonded together. Table 2.2 shows the melting point of the

material we used in designing. Cured PDMS will not melt at all while resin starts melting at 40 degrees. It can be concluded that only PLA and PMMA can be fixed together with thermal bonding.

Material	PLA	PMMA	PDMS	Resin	Glass
Melting point $/^{\circ}C$	150	160	N/A	N/A	1700

Table 2.2: The melting point of the candidate materials[7]

A pair of aluminum plates are designed for thermal bonding as figure 2.11 illustrates. The plates could withstand high temperatures and offer pressure during heating by the 4 bolts on each corner. The metal plates have a poor affinity to the plastic materials applied in the design. Hence, the design will be easily separated from the clamp after the bonding process without unexpected adhesion to the plate.

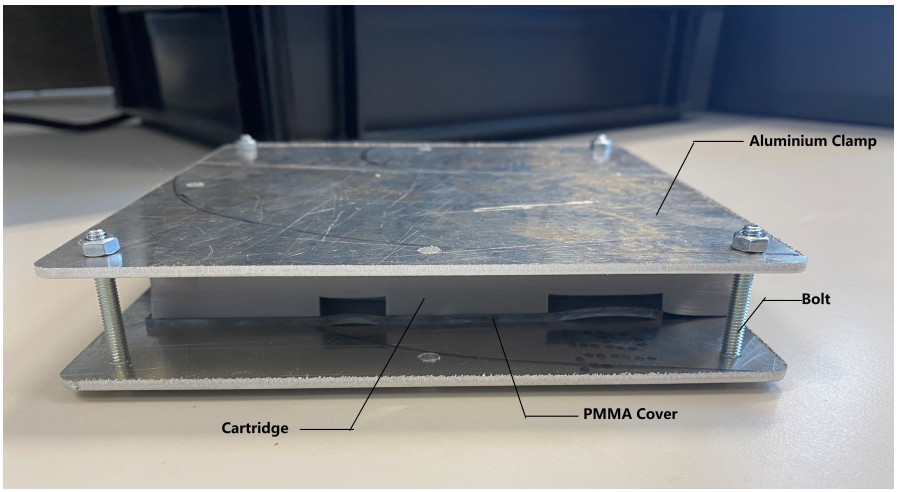

Figure 2.11: The illustration of a pair of aluminum thermal clamps. The two plates clamp the cartridge and the cover together to force the formation of bonding. The four bolts provide the necessary pressure for the process.

Another handy method is to use glue. There are a variety of glues for different materials and it would be a long article to explain the principles of different glues but glue is the most general bonding strategy both in daily life and industrial designs.

A very common method specially designed for PDMS material applied in microfluid experiments is surface activation. It relies on UV, Ozone, or Oxygen plasma to activate the function group on the surface of PDMS, forming covalent bonding with the target substrate [20].

Apart from the mentioned method in the previous paragraphs. There are still methods specifically designed for certain materials. For example, UV and ethanol are also applicable in PLA and PMMA in a different manner as shown in figure 2.12. Ethanol dissolves a small part of the contact surface for both materials, forming crosslinking of functional acrylate monomers from both substrates under UV exposure.

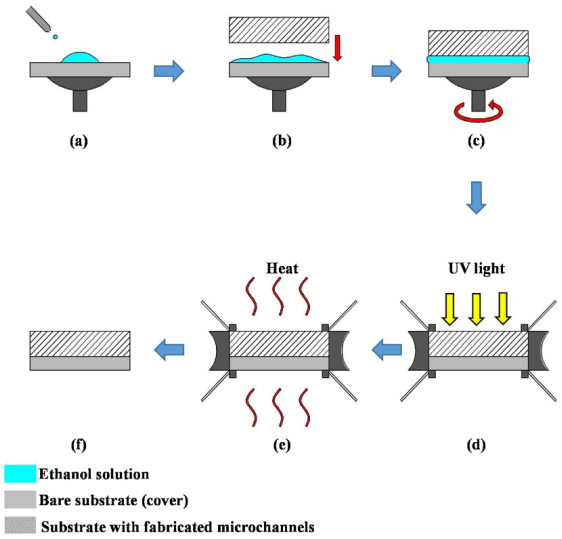

Figure 2.12: UV bonding method of PLA and PMMA:(a) manual pipette used to load ethanol solution on bare substrate; (b)substrate with fabricated microchannel brought into contact with bare substrate; (c)spin-coating for uniformed distribution of ethanol solution; (d) UV irradiation;(e)post-annealing for relief of residual stress; (f) bonded microfluidic chip.[6]

2.3.4 Evaluation of material selection and bonding method

The bonding method and material selection are closely related and by no means can they be discussed separately. In this section, a few combinations of material selection and bonding strategies are discussed and evaluated in this part.

The criteria of the evaluation include some of the challenges in chapter 2.2 like durable bonding, flat and transparent cover, and no glare. A few challenges that arise from the fabrication process like printing quality and hydrophilicity are also taken into consideration.

To ensure a smooth liquid flow when adding liquid, the hydrophilicity of the cartridge material should be noticed. The matrix 2.3shows the hydrophilicity of the cartridge materials offered by the lab measured by the water contact angle. The larger the angle, the more hydrophobic the material features, and the more resistance to liquid flow. It can be concluded that resin wins out with its best hydrophilicity.

Cartridge Material	PLA	PETG	Resin
Contact Angle °	60	75	55

Table 2.3: The contact angle of the cartridge materials[8]

After discussing the hydrophilicity of cartridge material, the printing quality of the materials should be compared as well. A prototype of PLA cartridge is fabricated. As is shown in figure 2.13, the surface of the fluid channel is rough with fibers of residue material and the arch-shape inlets of chambers are in bad shape. This may be contributed to impure material and a cold

nozzle during 3d printing. The fibers and the distorted structure prevents liquid from flowing freely because of the hydrophobic material. Similar fibers are found in the prototype printed from PETG It is considered to use physical and chemical methods to clean the fibers and to

Figure 2.13: The fibers on the surface of the cartridges. The fibers are mainly found around perpendicular structures.

Figure 2.14: The cartridge after the saturation in ethanol. The red colorant is the marker for the next step experiment.

Figure 2.15: The white residue concentrates on the surface of the cartridge after drying, making the cartridge unusable.

polish the rough surface. It is very common in commercial 3D printing to use organic solvent to remove printing defects[21]. Guided by this idea, a prototype is saturated in ethanol for 10 minutes in order to improve printing quality. The fibers are removed as shown in figure 2.14. The cleaning proves to be effective but it is troublesome to clean the half-dissolved material residue in the deep chambers. The white residue observed in figure 2.15 proves to be disastrous to the generation of the bonding with the cover. In regard to this disadvantage, we give up the idea of cleaning the fibers.

As the previous paragraphs show that the PLA and PETG materials have poor] performance in printing quality, a resin model by lithography is fabricated by photo-lithography. It features a smooth surface as figure 2.16 shows.

Besides hydrophilicity and printing quality, glare is another crucial problem we face during measurement. Glare describes the phenomenon of the object being illuminated by both reflected light and transmitted light. The glare problem frequently happens with light path penetrating multiphase of reflective material. The reflection rate of the material describes the seriousness of the glare problem. The more light penetrates through the cover, the less light is reflected between the mediums thus less severe the glare problem is. Because of this, the material of the cover is also changed from PMMA to glass because the glass has a smaller reflection rate (4% for glass[22] to 8% for PMMA[23]) in the visible spectrum.

Based on the discussion above, the morphology table is shown here in table 2.4. The table lists the material of the cartridge and the cover with the corresponding bonding method. Most of the bonding features with good quality in durability. The prototypes of thermal and glue bonding are examined one week after the bonding and they are still intact. As for the surface

Figure 2.16: A prototype printed by resin material with very smooth surface

activation method, it has less tensile strength when bonding with polymers compared to other methods[20]. Besides the poor strength, surface activation requires strong oxide or radiation treatment, which is catastrophic to the antibiotics inside the cartridge. In the same way, thermal bonding of around $150°C$ will greatly reduce the efficacy of the antibiotic.

From the aspects of performance, resin with glass is the best choice. However, the only disadvantage of this choice is that the resin printer in our lab has limited printing volume, allowing only 3 chambers on one cartridge.

Cartridge	Cover	Bonding	Durability	Printing quality	Hydrophilicity	Transparency	Glare	Avg
PETG	PMMA	Thermal	4	1	1	3	4	2.6
PLA	PMMA	Thermal	4	1	3	3	4	3
PLA	PDMS	Surface activation	1	1	4	1	4	2.2
Resin	PMMA	Glue	4	5	5	3	4	4.2
Resin	Glass	Glue	4	5	5	5	5	4.8

Table 2.4: The morphology table of fabrication

2.3.5 Determination of critical dimensional parameters

The previous section has determined the materials and the fabrication process of the design. Yet another few parameters matter a lot to some of the requirements. In this section, we will talk about the cylinder design to reduce glare, the wall thickness to improve the durability of the bonding, and the cross-section of the channel to avoid blockage.

First, the thickness of the wall is increased from 1mm to 2mm, increasing the contact area of the bonding. The quality of the bonding is tested right after finishing the bonding and 3 days later to test if the bonding is durable enough. The result shows that no leakage is detected 3 days later so the bonding durability is increased by enlarging the contact area.

It should be noticed that the larger the cartridge, the less influence the printing quality has on the liquid flow. However, it is unwise to increase the size of the cartridge to large enough to ignore the printing defects because of considerations in cost and volume. A series of prototypes

with different sizes are shown in table 2.5. It proves that a channel with a $5 * 5mm^2$ cross-section and the inlets of the chambers with a diameter of 5mm has the best balance between material cost and liquid flow.

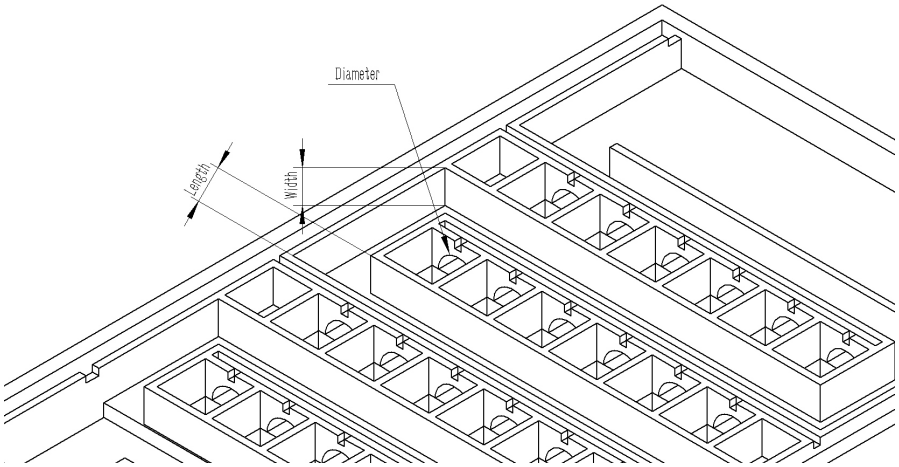

Figure 2.17: A picture to illustrate the important parameters of cross-section including width and length of the channel, the diameter of the arch-shaped inlet

Width	10	10	10	5	5
Length	5	5	5	2.5	5
Diameter	2	5	8	5	5
Performance	Blocked	Good	Good	Blocked	Good

Table 2.5: The changes of parameters and the performance of the cartridge

It is less meaningful to find out the smallest channel size without blockage. The design needs to be validated for its main function before optimizing its parameters. In conclusion, a 5*5mm cross-section with a 5mm half-round inlet is adopted.

Another idea to reduce glare while observing is to reduce the distance between the cover and the chip. A cylinder rises from the bottom of the chamber to raise the chip, reducing the distance between the cover and the chip from 7mm to 2mm. In the same way, the cylinder design will reduce the layer of liquid between the chip and the microscope, reducing the amount of transmitted light. The comparison is shown in figure 2.18.

In conclusion, the cartridge is made from resin with a ventilation channel while the glass cover is glued to the cartridge to seal the space. The design fulfills the function of liquid distribution and the requirement of durability. A photo of the final design is shown in figure 2.20.

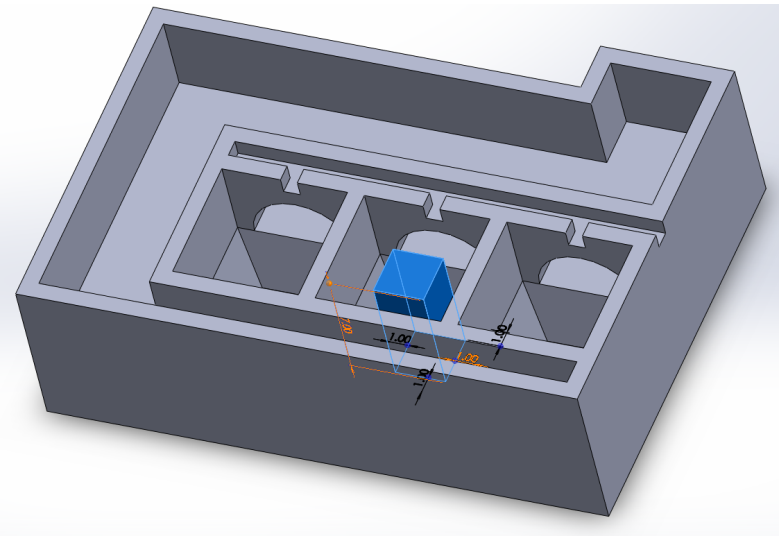

Figure 2.18: The illustration of the pillar used to reduce the glare. The pillar is colored blue in the center.

Without cylinder. Distance between cover and the chip: 7mm

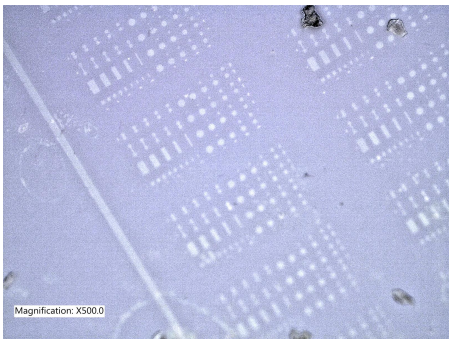

With cylinder. Distance between cover and the chip: 2mm

Figure 2.19: The comparison between the figures with and without cylinder design under Keyence microscope. The previous design without a cylinder has poor contrast under the microscope. Features of cavities and boundaries could barely be observed. When the cylinder design is applied, with the reduced distance between the chip and the cover, the glare problem is inhibited and a clear contrast of cavities and boundaries could be observed.

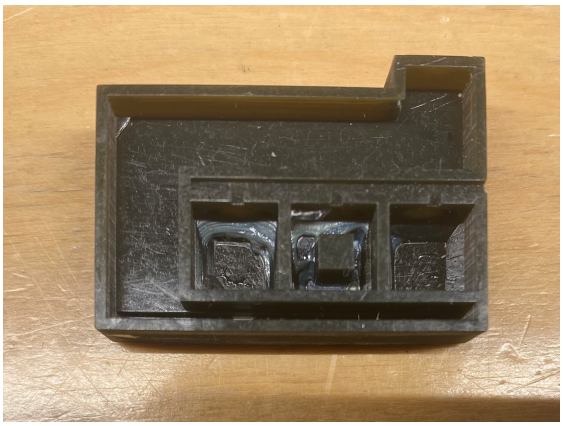

Figure 2.20: A photo of the final design. A chamber is designed with a cylinder. The other 2 chambers are empty as the control group.

Chapter 3

Performance validation

In the previous section, we analyzed the requirements of the design and determined what the design will be like in concept. Prototypes that satisfy the requirements are fabricated. After the design and fabrication process, this section will focus on the performance of the design during the measurement process.

The measurement process can be divided into several steps. After receiving a well-packaged cartridge with chips, drops of bacteria suspension will be inoculated into the cartridge first. Then the cartridge will be loaded on the optical setup and laser beam will focus on the cavity on the chip. Data of vibration can be acquired with an oscilloscope. The workflow of the measurement can be summarized in figure 3.1.

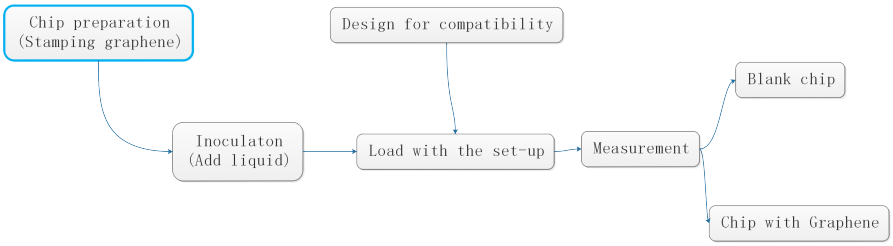

Figure 3.1: The workflow of the measurement process. The blue box of chip preparation is not the focus of this thesis. The validation process will start with Inoculation.

3.0.1 Inoculation

This section of the thesis will explain the step of inoculation. Experiment records of the inoculation step could validate the function of the fluid system design. Before adding liquid, the cartridge is placed vertically since the flow is driven by gravity. As an early validation experiment, it is not necessary to inoculate bacteria on the chip since the primary purpose of this experiment is about the fluid system. Instead of bacteria suspension, the liquid with colorant is injected into the cartridge by a pipette through the inlet on the top of the cartridge. It can be observed that with the liquid flowing, the chambers are fulfilled one by one. For a cartridge with 3 chambers, 6ml suspension is sufficient to fulfill all the chambers. Because of careful control

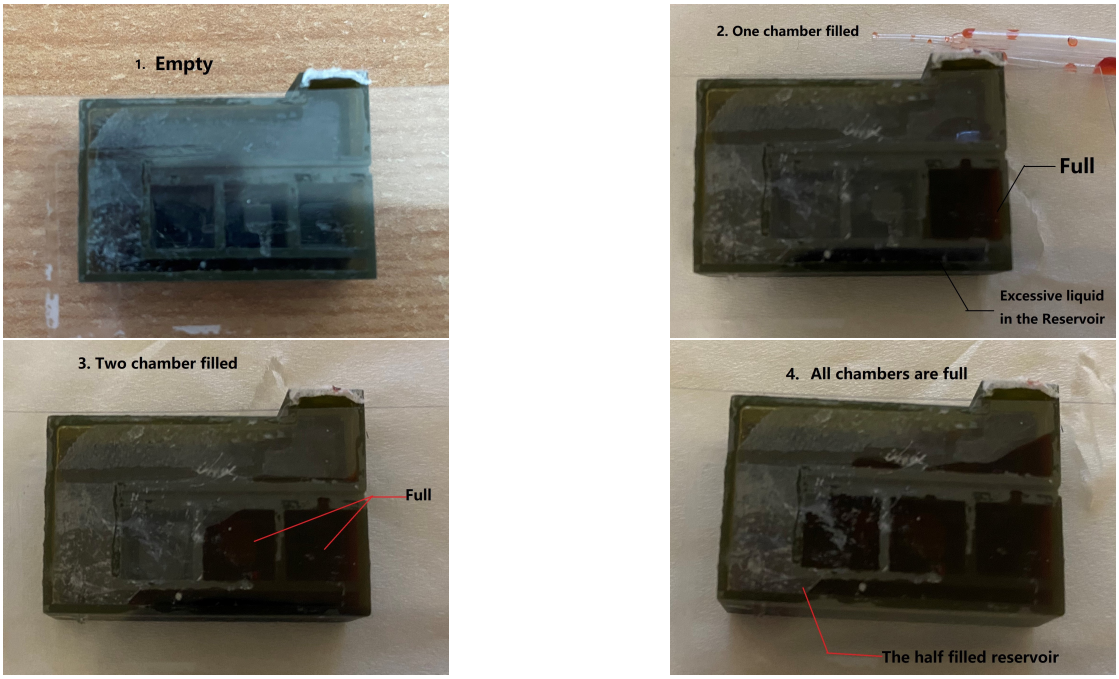

Figure 3.2: The photos of the inoculation process. The red-colored liquid enters from the top and fulfills each chamber one by one. The excessive liquid will flow to the bottom reservoir.

of the amount of liquid, there is little residual liquid left. The liquid can be found only in the bottom of the cartridge where the reservoir is designed.

The experiment shows that the design successfully distributes an equal amount of liquid into each chamber. Apart from functioning properly, the bonding of the two parts is firm and no leakage is detected. Bubbles generated during the process are expelled by the ventilation system. In addition, because there is little residual liquid left in the channel, the cross-contamination of different chambers is avoided.

3.0.2 Assembly with the setup and compatibility design

After the liquid was added, the cartridge was loaded on the setup. The prototype was placed on a nano-positioner before the objective as figure 3.3 illustrates.

Figure 3.3: The nano-positioner loaded with a cartridge. The surface of the platform is smooth and a plastic stage is 3D-printed and fixed on the surface with bolts to carry the cartridge moving with the platform.

The nano-positioner is controlled by 3 step motors with high resolution. The platform on the nano-positioner is able to move in 6 degrees of freedom. To assemble the nanopositioner with the cartridge, a compatible holder design is necessary to fix the cartridge to the platform. As figure 3.5 illustrates, a simple holder design could fulfill the task of connection. The holder is

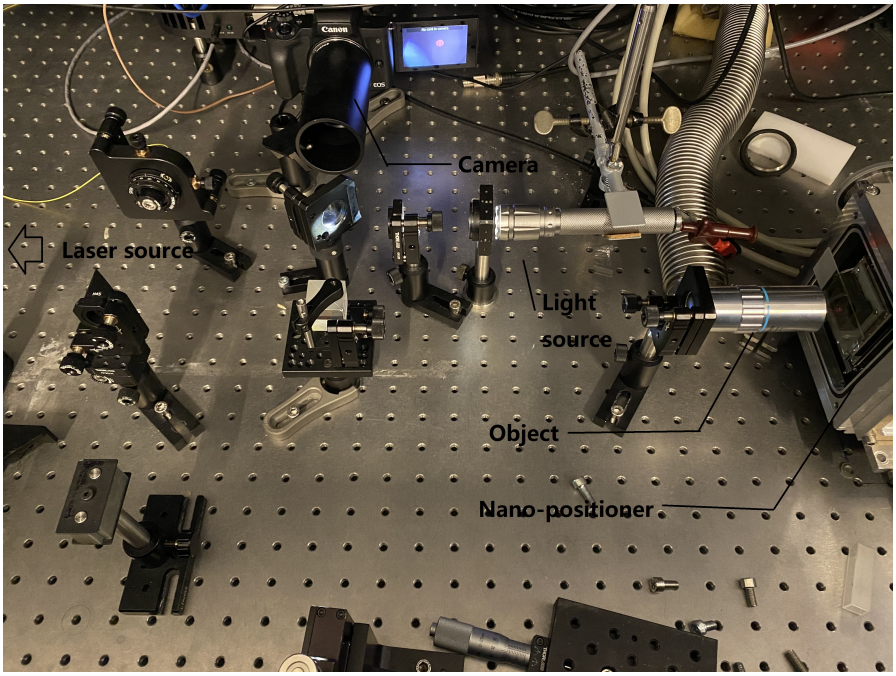

Figure 3.4: The real Enigma setup designed by Roslon et al in this research. The principle of the setup is introduced in chapter 1.

supposed to clamp the cartridge firmly while the platform is moving. A few designs with clamps was tested but the large glass slide sealing over the cartridge impede a firm design in space. At present, the friction between the cartridge and the holder could withstand the pulse when the platform moves and stops. In regard to this, the experiment could continue with a holder like this.

As a design for compatibility, it is not necessary to devote too much effort to the holder because the setup and the cartridge may be improved during the experiment. The final design of the holder may be determined when the cartridge is applied to clinical analysis.

3.0.3 Vibration measurement

After verifying the fluid flow function in the cartridge and the mounting of the cartridge on the setup, the design could be finally tested under the optical setup. First, the cartridge will be observed under the Keyence microscope to have a clear view of the cavities because the camera in the setup has poorer image quality. After proving that the chip is well-placed inside the cartridge, the prototypes can be tested finally under the setup and vibrations of the graphene drum are measured. As a control group, the vibration of blank chips without graphene is also measured.

Measurement of blank chips A prototype loaded with blank chips without graphene is fabricated as the control group. The chips are observed under the Keyence microscope and measured under the setup. Figure 3.6 compares the image quality before and after adding the

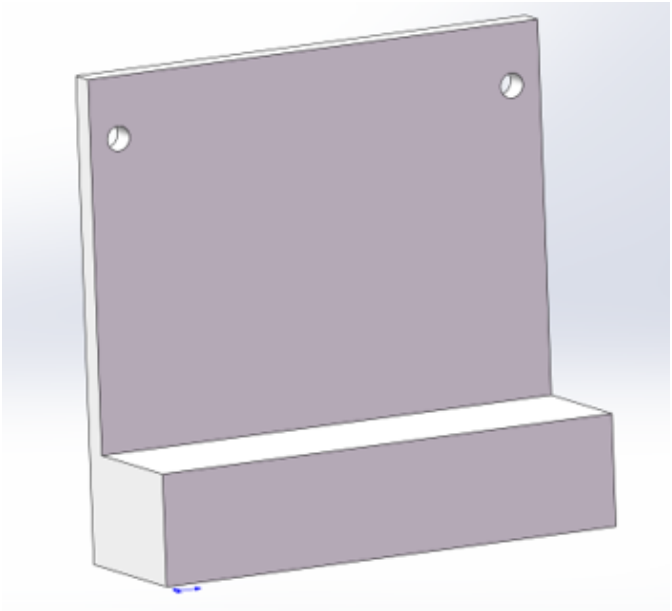

Figure 3.5: The holder designed for the mounting of the cartridge The two holes correspond to the threaded hole on the nano-positioner for mounting

liquid. Although after adding liquid, the image quality is worse than the one without liquid, the picture is clear enough to recognize the cavities thanks to post-processing and the cylinder.

After observing a clear view of the cavities, the laser beam is aimed at one cavity to measure the reflected signal as figure 3.7 shows. 16 cavities on each chip are measured for 30 seconds before and after adding the liquid. A pair of the signal charts in figure 3.8 shows that the voltage of the photodiode received from the reflected laser is similar to the power of the direct laser, 150mV and 220mV. The variance σ is small indicating that only blank noise is detected. The power spectral density(PSD) figure shows the characteristic of the signal in the frequency domain. Currently, the PSD chart is meaningless since only white noise is recorded. According to Roslon's work, it will make a difference when bacteria is added.

Measurement with graphene drum Another prototype is stamped with graphene as figure 3.9 shows. The cavities with the graphene drum are carefully measured in the setup. The image under this setup has worse quality than the one taken under the Keyence microscope because the camera in the setup has a lower definition. The signal features no difference from the previous group without graphene as figure 3.10 shows. Although improved in image quality to fight against the glare problem, it is still difficult to have a clear view of the cavity after adding the liquid, making it harder to aim the laser at the center of the cavity. As figure 3.11 illustrates, compared to the pictures without liquid, the cavities could barely be observed in the setup because of poor contrast. The measurement is halted because of failure to aim at the cavity.

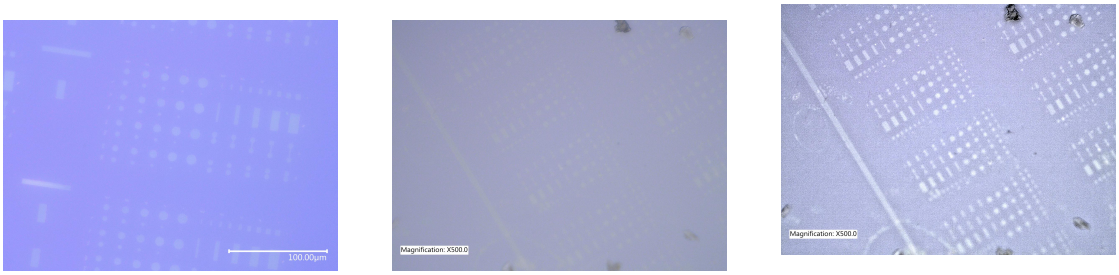

Before adding liquid (500X) | After adding liquid (500X) | After adding liquid(post-process)

Figure 3.6: The image quality of the chip without graphene under Keyence Microscope. Arrays of cavities are clearly observed before adding liquid. After adding the liquid, the image is brighter than expected because of the glare problem so the contrast of the picture is post-processed to increase its readability as the figure shows.

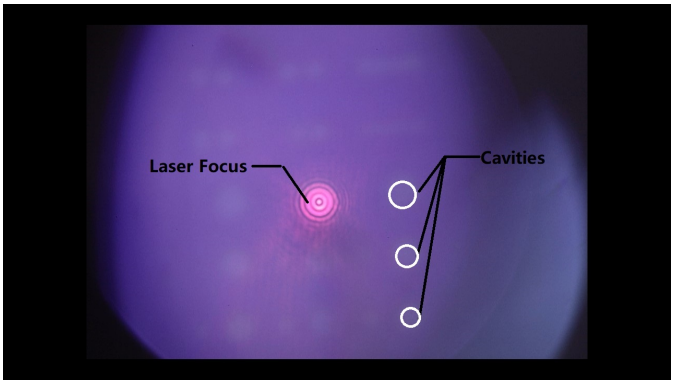

Figure 3.7: The laser is pointing at the center of a cavity. Some cavities are stressed with white circles

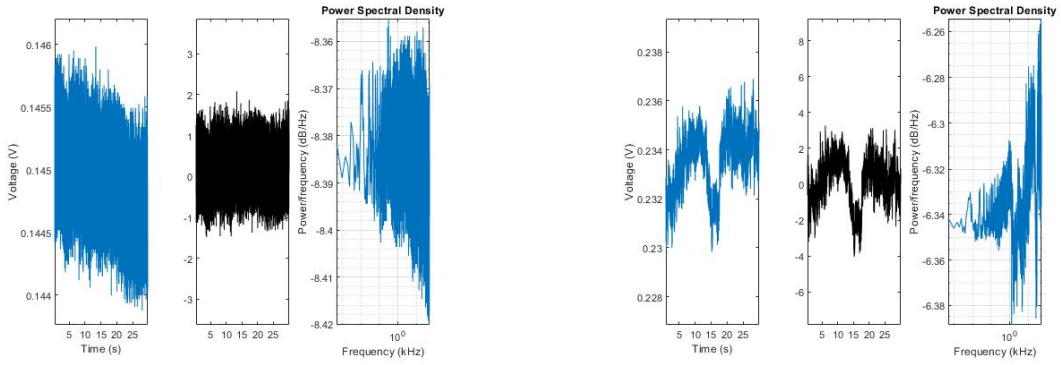

The signal before adding liquid | The signal after adding liquid

Figure 3.8: The signal comparison before and after adding the liquid. The signal is represented with 3 plots, voltage to time, amplitude to time, and Power spectral density. The data shows little variance indicating only blank noise.

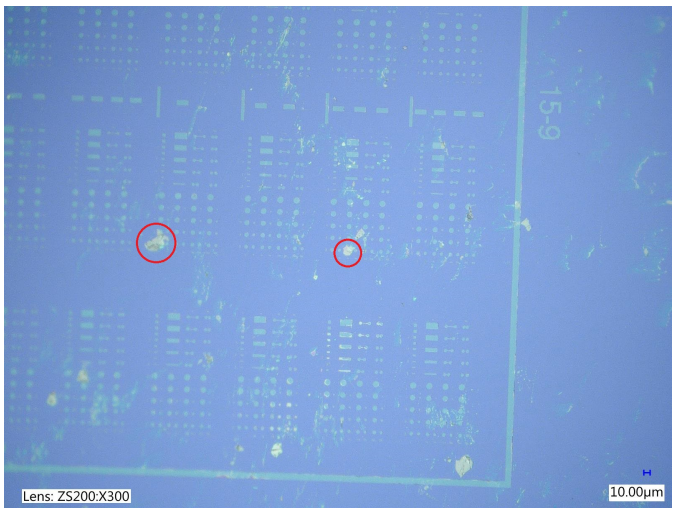

Figure 3.9: The microscope image of cavities with graphene membrane. The cavities stamped with graphene are pointed out with red circles.

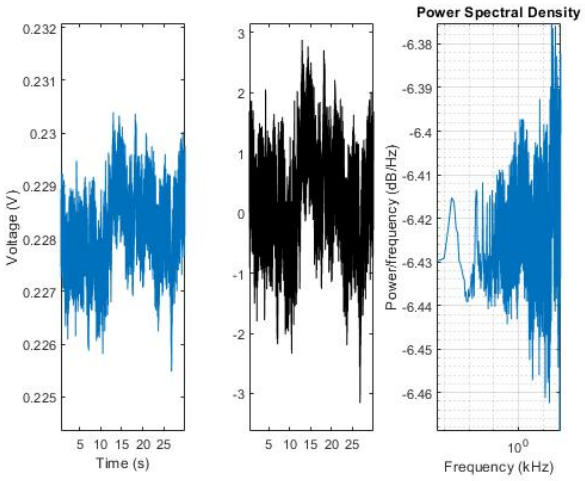

Figure 3.10: The received signal of graphene drum

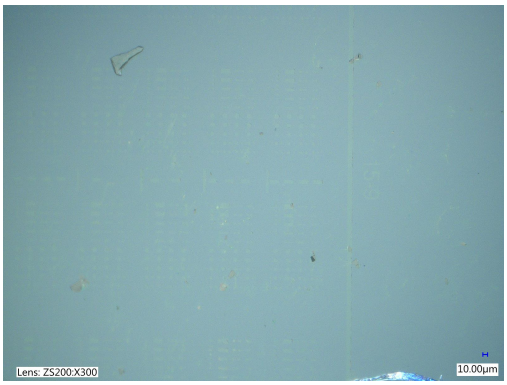

The chip with graphene saturated in liquid observed under Keyence Microscope

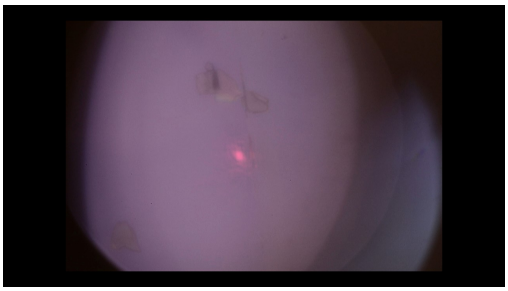

The cavity with graphene saturated in liquid observed in the setup

Figure 3.11: The pictures taken by Keyence microscope and the setup. Both of the pictures are blurred because of glare problems.

Chapter 4

Conclusion and Outlook

In the last chapter, the design proves to be feasible by validation experiment of its two main functions, fluid flow and optical measurement. Most of the obstacles during the experiment are overcome while some problems partially remain. This chapter will conclude the experiments and discuss the possible improvement in the future.

4.1 Resolving the research question

The research question driving this design is rephrased here: how to design a device that carries out parallel nanomotion AST measurements with different antibiotics and concentrations at one time?

For this purpose, a cartridge with different chambers is designed for the chips loaded with graphene drums. Freeze-dried antibiotics and chips are placed inside the chambers before the cartridge is sealed. A zig-zag channel on the cartridge is supposed to distribute the required liquid to each chamber. The cartridge is designed to be compatible with the setup of the nanomotion method and precise measurement data of different antibiotics and concentrations can be acquired from a one-time measurement.

The fabrication process of the design is simple without high requirements of instruments. The design is highly integrated and automated so most of the fabrication and measurement steps could be processed by machines. Compared to the competitor products mentioned in the introductory chapters, this design adopts nanomotion methods which require little incubation time (around 1h). Compared to the first research on the nanomotion method by Rolson et.al, the design features parallel measurements which greatly improves the efficiency when applying the method to clinical diagnosis.

4.2 Reflection and Outlook

We have acknowledged the achievement of the cartridge design in the previous part but it is still far from a reliable and low-cost AST method application. This section will summarize the design and validation process in this thesis and reflect on the research. The design will be

evaluated from several aspects in this section. First, the dimensional parameters of the design could be optimized based on simulation. Second, the glare problem is still the greatest obstacle that influences the view under the microscope. As an application to clinical analysis, the design should be improved for mass production in its fabrication and measurement steps.

4.2.1 Simulation and optimization

To prove that the prototype functions well in distributing liquid, it is also considered to use fluid flow simulation before the validation experiments. A multi-phase simulation considering hydrophobic wall material and air flow would represent the model properly. Additionally, the prototype should concern practical matters including hydrophilicity and printing quality, of which the simulation requires a more complex model. It is unwise to spend much time finding a proper representative simulation model. Instead, the simulation process is skipped and prototypes are fabricated to prove their function practically.

Apart from this, the simulation could still be utilized in the future to optimize the parameters in order to save material while maintaining the performance of the cartridge. For example, the channel geometric parameters are discussed in chapter 2.3.5 and only a few parameters are tested. With the help of simulation, the most suitable parameters could be determined for the future production.

4.2.2 Material selection

Apart from the complex simulation conditions to validate the fluid system, the dimensional parameters of the prototype are larger than usual because of the hydrophobic material, requiring more liquid than expected to ensure the measurement. In the future, another proper simulation model is expected to optimize this model for more chambers and better performance. When material and fabrication are permitted, the prototype could be designed more compactly with more chambers based on the optimization process.

Another problem with the material has been mentioned in Chapter 2.3. Because of the restriction in the printing volume of lab instruments, only a design with 3 chambers is fabricated and validated. According to the manual for AST[10], around 10 antibiotics and 3 different concentrations of each kind should be tested against an unknown sample. In this case, the design with 3 chambers is far from enough to satisfy the analysis requirement. In the future, a larger-scale design with more chambers should be fabricated with a resin printer of large printing volume.

The last problem with the material is color. As we can see from figure 3.2, the deep-color resin material features very bad image quality both in photos and microscope images. Transparent or material with light color will significantly improve usability during the observation process. In another word, the cartridge in light color could be observed clearly with the naked eye and microscope. It will be much easier for the technicians to distinguish empty cartridges from full ones. A prototype was fabricated from transparent resin once during the experiment but the choice is abandoned because the stiffness of the resin type is not good enough. For better performance in the future, the material of the cartridge should take the color problem into consideration.

4.2.3 Alignment and Calibration

The design in the thesis adopts multiple chambers to place the chips. After finishing the measurement of the previous chip, the nano-positioner is required to move a long range to the next chamber for the laser beam to focus on the next chip. Compared to the average distance between cavities of 25 μm, the distance between the chips is 7 mm in the design. If the chips are not carefully aligned, long-distance movement of the stage would impede the laser beam from focusing on the cavities of the next chip. In this case, calibration is required when between measurements of different chips in the same cartridge, wasting precious time and labor.

To avoid frequent calibration during the measurement, there are generally two ways. The first method is to carefully bind the chip to the chamber with little installation error. Another method is to compensate for the error automatically in the control program of the nano-positioner. Both methods would be of great help to the improvement of the design in the futrue.

4.2.4 Glare

The glare problem is very common in a multiphase light path as we have discussed the reason in chapter 2.3. In our observation, it is unavoidable for light to penetrate several layers of air, solid material, and liquid.

Such a problem prevents the verification of the nanomotion method because of poor image quality. For example, in chapter 3, the measurement against graphene drums is not successful because of the glare problem. The glare results in an obscure view when calibrating the laser beam. Several methods regarding material and design have been adopted to reduce the influence of glare problems in this thesis, for example, cylinder design and material selection but they are far from enough.

There are generally two ways to solve the problem. The first one is to improve the illumination part of the setup. In our setup, the focus of the torch is moving with the focus of the laser. If the focus of the torch could move individually along the light axis, the glare problem could be avoided[24]. From another aspect of photography, applying a polarizer to the light source could also help to solve the problem. From the aspect of design, there is still much that could be improved. The thinner cover should be the first option to consider. During the experiment, cartridges sealed with PMMA cover of 2,1 and 0.5mm thickness are observed under the Keyence microscope. It proves that the thinner the cover, the less serious the glare problem is. However, the thinner cover has poor strength and the surface is not flat enough to meet the requirement. For the next-generation design, a thinner flat cover should be the best choice.

In the future, apart from the improvement in material and design, more improvements should be taken into consideration like improving the resolution, applying a polarizer, and moving the focus of the illumination focus. These possible solutions in optics offer a new direction for improving the design.

4.2.5 Mass production

As an attempt to apply a novel technique to clinical analysis, the cartridge is expected to be designed and fabricated with cheap, reliable production methods. In the thesis, the main parts of the cartridge are fabricated with 3d-printing and materials everywhere. However, the assembly

and the measurement process are still completed by manual work. In the future, most of the tasks during fabrication and measurement should be carried out automatically with a standard process in order to reduce the in-hand time of technicians.

In conclusion, the design presented by this thesis fulfills the task of carrying parallel nanomotion method AST measurement for clinical analysis and diagnosis with advantages to the clinical methods currently applied. The design still needs improvement in parameter optimization for a compact design, fabrication for mass production, and its corresponding optical setup.

Acknowledgement

Foremost, I would like to express my sincere gratitude to my supervisors prof.dr.Farbod Alijani, ir.Irek Roslon, dr.ir.Aleksandre Japaridze for the continuous support of my master's study and research, and for their patience, motivation, enthusiasm, and immense knowledge. Their guidance helped me in all the time of research and writing of this thesis. I could not have imagined having better mentors.

I would like to thank my fellow labmates, Victor Struijk, Santiago Mendoza Silva for their help and advice during my work on my master's thesis.
In addition, I would like to thank the lab technicians for providing aid and training for the instruments. They have offered valuable advice on fabrication and improvements

Last but not the least, I would like to thank my family and my friends for their support and encouragement during the two years.

Bibliography

[1] J. M. Andrews, "Determination of minimum inhibitory concentrations," *Journal of antimicrobial Chemotherapy*, vol. 48, no. suppl_1, pp. 5–16, 2001.

[2] G. Longo, L. Alonso-Sarduy, L. M. Rio, A. Bizzini, A. Trampuz, J. Notz, G. Dietler, and S. Kasas, "Rapid detection of bacterial resistance to antibiotics using afm cantilevers as nanomechanical sensors," *Nature Nanotechnology*, vol. 8, pp. 522–526, 2013.

[3] I. Roslon, A. Japaridze, P. G. Steeneken, and F. Alijani, "Probing nanomotion of single bacteria with graphene drums," *bioRxiv*, vol. 461186, 2021.

[4] C. G. Yang, Y. F. Wu, Z. R. Xu, and J. H. Wang, "A radial microfluidic concentration gradient generator with high-density channels for cell apoptosis assay," *Lab on a Chip*, vol. 11, pp. 3305–3312, 10 2011.

[5] A. M. Taylor, S. Menon, and S. L. Gupton, "Passive microfluidic chamber for long-term imaging of axon guidance in response to soluble gradients," *Lab on a Chip*, vol. 15, pp. 2781–2789, 7 2015.

[6] H. D. Lynh and C. Pin-Chuan, "Novel solvent bonding method for creation of a three-dimensional, non-planar, hybrid pla/pmma microfluidic chip," *Sensors and Actuators, A: Physical*, vol. 280, pp. 350–358, 9 2018.

[7] "Melting point." https://en.wikipedia.org/wiki/Melting_point#, Jan. 2023.

[8] S. Kim, "Fibres and polymers," *Vol. 7 (3)*, pp. 255–261, 2006.

[9] "Antimicrobial resistance global report on surveillance: 2014 summary," tech. rep., World Health Organization, 2014.

[10] S. Cavalieri and A. S. for Microbiology, *Manual of Antimicrobial Susceptibility Testing*. American Society for Microbiology, 2009.

[11] K. Syal, M. Mo, H. Yu, R. Iriya, W. Jing, S. Guodong, S. Wang, T. E. Grys, S. E. Haydel, and N. Tao, "Current and emerging techniques for antibiotic susceptibility tests," 2017.

[12] P. Stupar, O. Opota, G. Longo, G. Prod'hom, G. Dietler, G. Greub, and S. Kasas, "Nanomechanical sensor applied to blood culture pellets: a fast approach to determine the antibiotic susceptibility against agents of bloodstream infections," *Clinical Microbiology and Infection*, vol. 23, pp. 400–405, 6 2017.

[13] C. Lissandrello, F. Inci, M. Francom, M. R. Paul, U. Demirci, and K. L. Ekinci, "Nanomechanical motion of escherichia coli adhered to a surface," *Applied Physics Letters*, vol. 105, 9 2014.

[14] J. Mertens, A. Cuervo, and J. L. Carrascosa, "Nanomechanical detection of: Escherichia coli infection by bacteriophage t7 using cantilever sensors," *Nanoscale*, vol. 11, pp. 17689–17698, 10 2019.

[15] S. Kasas, F. S. Ruggeri, C. Benadiba, C. Maillard, P. Stupar, H. Tournu, G. Dietler, and G. Longo, "Detecting nanoscale vibrations as signature of life," *Proceedings of the National Academy of Sciences of the United States of America*, vol. 112, pp. 378–381, 1 2015.

[16] A. Mustazzolu, L. Venturelli, S. Dinarelli, K. Brown, R. A. Floto, G. Dietler, L. Fattorini, S. Kasas, M. Girasole, and G. Longo, "A rapid unraveling of the activity and antibiotic susceptibility of mycobacteria," *Antimicrobial Agents and Chemotherapy*, vol. 63, 3 2019.

[17] A. C. Kohler, L. Venturelli, A. Kannan, D. Sanglard, G. Dietler, R. Willaert, and S. Kasas, "Yeast nanometric scale oscillations highlights fibronectin induced changes in c. albicans," *Fermentation*, vol. 6, 2020.

[18] A. Japaridze, E. Orlandini, K. B. Smith, L. Gmür, F. Valle, C. Micheletti, and G. Dietler, "Spatial confinement induces hairpins in nicked circular dna," *Nucleic Acids Research*, vol. 45, pp. 4905–4914, 5 2017.

[19] J. Diao, L. Young, S. Kim, E. A. Fogarty, S. M. Heilman, P. Zhou, M. L. Shuler, M. Wu, and M. P. DeLisa, "A three-channel microfluidic device for generating static linear gradients and its application to the quantitative analysis of bacterial chemotaxis," *Lab on a Chip*, vol. 6, pp. 381–388, 2006.

[20] A. Borók, K. Laboda, and A. Bonyár, "Pdms bonding technologies for microfluidic applications: A review," 8 2021.

[21] "Smoothing pla 3d prints with sandpaper, solvents, and more." https://www.wevolver.com/article/smoothing-pla-3d-prints-with-sandpaper-solvents-and-more, Mar. 2022.

[22] "Optical properties of glass: How light and glass interact?." https://www.koppglass.com/blog/optical-properties-glass-how-light-and-glass-interact.

[23] M. Burghoorn, D. Roosen-Melsen, J. Riet, S. Sabik, Z. Vroon, I. Yakimets, and P. Buskens, "Single layer broadband anti-reflective coatings for plastic substrates produced by full wafer and roll-to-roll step-and-flash nano-imprint lithography," *Materials*, vol. 6, pp. 3710–3726, 09 2013.

[24] W. T. Dempster, "Principles of microscope illumination and the problem of glare," 1944.

[25] K. Rogers, "Bacteria."

[26] D. Lu, Q. Jiang, M. Zheng, J. Zhang, Y. Huang, and B. Hou, "The role of ammonium chloride in the powder thermal diffusion alloying process on a magnesium alloy," *Coatings*, vol. 9, 4 2019.

[27] S. H. Strogatz, "Sync: The emerging science of spontaneous order."

[28] R. Casasola, N. L. Thomas, A. Trybala, and S. Georgiadou, "Electrospun poly lactic acid (pla) fibres: Effect of different solvent systems on fibre morphology and diameter," *Polymer*, vol. 55, pp. 4728–4737, 9 2014.

[29] S. H. Lee and S. Y. Yeo, "Improvement of hydrophilicity of polylactic acid (pla) fabrics by means of a proteolytic enzyme from bacillus licheniformis," *Fibers and Polymers*, vol. 17, pp. 1154–1161, 8 2016.

[30] A. Palitsch, M. Hannig, P. Ferger, and M. Balkenhol, "Bonding of acrylic denture teeth to mma/pmma and light-curing denture base materials: The role of conditioning liquids," *Journal of Dentistry*, vol. 40, pp. 210–221, 3 2012.

[31] P. K. Vallittu, "Bonding of resin teeth to the polymethyl methacrylate denture base material," *Acta Odontologica Scandinavica*, vol. 53, pp. 99–104, 1995.

[32] M. Erickstad, L. A. Hale, S. H. Chalasani, and A. Groisman, "A microfluidic system for studying the behavior of zebrafish larvae under acute hypoxia," *Lab on a Chip*, vol. 15, pp. 857–866, 2 2015.

[33] A. K. Hosokawa, T. Fujii, and I. Endo, "Hydrophobic microcapillary vent for pneumatic manipulaiton of liquid in /ltas," 1998.

[34] S. Chung, H. Yun, and R. D. Kamm, "Nanointerstice-driven microflow," *Small*, vol. 5, pp. 609–613, 3 2009.

[35] K. T. L. Trinh, W. R. Chae, and N. Y. Lee, "Pressure-free assembling of poly(methyl methacrylate) microdevices via microwave-assisted solvent bonding and its biomedical applications," *Biosensors*, vol. 11, 12 2021.

[36] A. Olanrewaju, M. Beaugrand, M. Yafia, and D. Juncker, "Capillary microfluidics in microchannels: From microfluidic networks to capillaric circuits," 8 2018.

[37] P. Ertl, E. Robello, F. Battaglini, and S. R. Mikkelsen, "Rapid antibiotic susceptibility testing via electrochemical measurement of ferricyanide reduction by escherichia coli and clostridium sporogenes," *Analytical Chemistry*, vol. 72, pp. 4957–4964, 10 2000.

[38] T. S. Mann and S. R. Mikkelsen, "Antibiotic susceptibility testing at a screen-printed carbon electrode array," *Analytical Chemistry*, vol. 80, pp. 843–848, 2 2008.

[39] J. Choi, Y. G. Jung, J. Kim, S. Kim, Y. Jung, H. Na, and S. Kwon, "Rapid antibiotic susceptibility testing by tracking single cell growth in a microfluidic agarose channel system," *Lab on a Chip*, vol. 13, pp. 280–287, 1 2013.

[40] M. O. Paraense, T. H. R. da Cunha, A. S. Ferlauto, and K. C. de Souza Figueiredo, "Monolayer and bilayer graphene on polydimethylsiloxane as a composite membrane for gas-barrier applications," *Journal of Applied Polymer Science*, vol. 134, 12 2017.

[41] T. Niu, G. Cao, and C. Xiong, "Indentation behavior of the stiffest membrane mounted on a very compliant substrate: Graphene on pdms," *International Journal of Solids and Structures*, vol. 132-133, pp. 1–8, 2 2018.

[42] U. Abidin, N. A. S. M. Daud, and V. L. Brun, "Replication and leakage test of polydimethylsiloxane (pdms) microfluidics channel," vol. 2062, American Institute of Physics Inc., 1 2019.

[43] K. Sun, J. Dong, Z. Wang, Z. Wang, G. Fan, Q. Hou, L. An, M. Dong, R. Fan, and Z. Guo, "Tunable negative permittivity in flexible graphene/pdms metacomposites," *Journal of Physical Chemistry C*, vol. 123, pp. 23635–23642, 9 2019.

[44] S. M. Kozlov, F. Viñes, and A. Görling, "Bonding mechanisms of graphene on metal surfaces," *Journal of Physical Chemistry C*, vol. 116, pp. 7360–7366, 4 2012.

[45] W. Jing, X. Jiang, W. Zhao, S. Liu, X. Cheng, and G. Sui, "Microfluidic platform for direct capture and analysis of airborne mycobacterium tuberculosis," *Analytical Chemistry*, vol. 86, pp. 5815–5821, 6 2014.

[46] C. Kim, J. H. Bang, Y. E. Kim, S. H. Lee, and J. Y. Kang, "On-chip anticancer drug test of regular tumor spheroids formed in microwells by a distributive microchannel network.," *Lab on a chip*, vol. 12, pp. 4135–4142, 2012.

[47] R. Iriya, W. Jing, K. Syal, M. Mo, C. Chen, H. Yu, S. E. Haydel, S. Wang, and N. Tao, "Rapid antibiotic susceptibility testing based on bacterial motion patterns with long short-term memory neural networks," *IEEE Sensors Journal*, vol. 20, pp. 4940–4950, 5 2020.

[48] B. Dai, Y. Long, J. Wu, S. Huang, Y. Zhao, L. Zheng, C. Tao, S. Guo, F. Lin, Y. Fu, D. Zhang, and S. Zhuang, "Generation of flow and droplets with an ultra-long-range linear concentration gradient," *Lab on a Chip*, 2021.

[49] J. Plutnar, M. Pumera, and Z. Sofer, "The chemistry of cvd graphene," 2018.

[50] K. B. Smith, M. Wehrli, A. Japaridze, S. Assenza, C. Dekker, and R. Mezzenga, "Interplay between confinement and drag forces determine the fate of amyloid fibrils," *Physical Review Letters*, vol. 124, 3 2020.

[51] T. J. Abram, H. Cherukury, C. Y. Ou, T. Vu, M. Toledano, Y. Li, J. T. Grunwald, M. N. Toosky, D. F. Tifrea, A. Slepenkin, J. Chong, L. Kong, D. V. D. Pozo, K. T. La, L. Labanieh, J. Zimak, B. Shen, S. S. Huang, E. Gratton, E. M. Peterson, and W. Zhao, "Rapid bacterial detection and antibiotic susceptibility testing in whole blood using one-step, high throughput blood digital pcr," *Lab on a Chip*, vol. 20, pp. 477–489, 2 2020.

[52] J. Choi, H. Y. Jeong, G. Y. Lee, S. Han, S. Han, B. Jin, T. Lim, S. Kim, D. Y. Kim, H. C. Kim, E. C. Kim, S. H. Song, T. S. Kim, and S. Kwon, "Direct, rapid antimicrobial susceptibility test from positive blood cultures based on microscopic imaging analysis," *Scientific Reports*, vol. 7, 12 2017.

[53] J. S. Bunch, A. M. V. D. Zande, S. S. Verbridge, I. W. Frank, D. M. Tanenbaum, J. M. Parpia, H. G. Craighead, and P. L. McEuen, "Electromechanical resonators from graphene sheets," *Science*, vol. 315, pp. 490–493, 1 2007.

[54] G. Tetz and V. Tetz, "Evaluation of a new culture-based atbfinder test-system employing a novel nutrient medium for the selection of optimal antibiotics for critically ill patients with polymicrobial infections within 4 h," *Microorganisms*, vol. 9, 5 2021.

[55] E. C. Reynoso, S. Laschi, I. Palchetti, and E. Torres, "Advances in antimicrobial resistance monitoring using sensors and biosensors: A review," 8 2021.

[56] L. Venturelli, Z. R. Harrold, A. E. Murray, M. I. Villalba, E. M. Lundin, G. Dietler, S. Kasas, and R. Foschia, "Nanomechanical bio-sensing for fast and reliable detection of viability and susceptibility of microorganisms," *Sensors and Actuators B: Chemical*, vol. 348, 12 2021.

[57] S. Kasas, A. Malovichko, M. I. Villalba, M. E. Vela, O. Yantorno, and R. G. Willaert, "Nanomotion detection-based rapid antibiotic susceptibility testing," 3 2021.

[58] M. I. Villalba, P. Stupar, W. Chomicki, M. Bertacchi, G. Dietler, L. Arnal, M. E. Vela, O. Yantorno, and S. Kasas, "Nanomotion detection method for testing antibiotic resistance and susceptibility of slow-growing bacteria," *Small*, vol. 14, 1 2018.

[59] N. Wadhwa and H. C. Berg, "Bacterial motility: machinery and mechanisms," 2021.

[60] I. Bennett, A. L. Pyne, and R. A. McKendry, "Cantilever sensors for rapid optical antimicrobial sensitivity testing," *ACS Sensors*, vol. 5, pp. 3133–3139, 10 2020.

[61] T. P. Burg, M. Godin, S. M. Knudsen, W. Shen, G. Carlson, J. S. Foster, K. Babcock, and S. R. Manalis, "Weighing of biomolecules, single cells and single nanoparticles in fluid," *Nature*, vol. 446, pp. 1066–1069, 4 2007.

[62] S. Aghayee, C. Benadiba, J. Notz, S. Kasas, G. Dietler, and G. Longo, "Combination of fluorescence microscopy and nanomotion detection to characterize bacteria," *Journal of Molecular Recognition*, vol. 26, pp. 590–595, 11 2013.

[63] H. Etayash, M. F. Khan, K. Kaur, and T. Thundat, "Microfluidic cantilever detects bacteria and measures their susceptibility to antibiotics in small confined volumes," *Nature Communications*, vol. 7, 10 2016.

[64] Y. Arntz, J. D. Seelig, H. P. Lang, J. Zhang, P. Hunziker, J. P. Ramseyer, E. Meyer, M. Hegner, and C. Gerber, "Label-free protein assay based on a nanomechanical cantilever array," 2003.

[65] C. Steffens, F. L. Leite, C. C. Bueno, A. Manzoli, and P. S. D. P. Herrmann, "Atomic force microscopy as a tool applied to nano/biosensors," 6 2012.

[66] P. Hinterdorfer and Y. F. Dufrêne, "Detection and localization of single molecular recognition events using atomic force microscopy," 5 2006.

[67] P. M. Kosaka, V. Pini, J. J. Ruz, R. A. D. Silva, M. U. González, D. Ramos, M. Calleja, and J. Tamayo, "Detection of cancer biomarkers in serum using a hybrid mechanical and optoplasmonic nanosensor," *Nature Nanotechnology*, vol. 9, pp. 1047–1053, 1 2014.

[68] M. Voumard, L. Venturelli, M. Borgatta, A. Croxatto, S. Kasas, G. Dietler, F. Breider, and U. V. Gunten, "Adaptation of: Pseudomonas aeruginosa to constant sub-inhibitory concentrations of quaternary ammonium compounds," *Environmental Science: Water Research and Technology*, vol. 6, pp. 1139–1152, 4 2020.

[69] A. S. Davydov, "The theory of contraction of proteins under their excitation," 1973.

[70] G. Longo, L. M. Rio, C. Roduit, A. Trampuz, A. Bizzini, G. Dietler, and S. Kasas, "Force volume and stiffness tomography investigation on the dynamics of stiff material under bacterial membranes," vol. 25, pp. 278–284, 5 2012.

[71] O. Malvar, J. J. Ruz, P. M. Kosaka, C. M. Domínguez, E. Gil-Santos, M. Calleja, and J. Tamayo, "Mass and stiffness spectrometry of nanoparticles and whole intact bacteria by multimode nanomechanical resonators," *Nature Communications*, vol. 7, 11 2016.

[72] G. Longo and S. Kasas, "Effects of antibacterial agents and drugs monitored by atomic force microscopy," 2014.

[73] L. Venturelli, A. C. Kohler, P. Stupar, M. I. Villalba, A. Kalauzi, K. Radotic, M. Bertacchi, S. Dinarelli, M. Girasole, M. Pešić, J. Banković, M. E. Vela, O. Yantorno, R. Willaert, G. Dietler, G. Longo, and S. Kasas, "A perspective view on the nanomotion detection of living organisms and its features," *Journal of Molecular Recognition*, vol. 33, 12 2020.